Istiyanti and Goto
Geoenvironmental Disasters (2022) 9:21
https://doi.org/10.1186/s40677-022-00223-4

Geoenvironmental Disasters

RESEARCH Open Access

Characteristics of physical properties of the sliding and its surrounding layers in landslides caused by the 2018 Hokkaido Eastern Iburi Earthquake

Mega Lia Istiyanti[1] and Satoshi Goto[2*]

Abstract

A 6.6-M_w earthquake struck the Iburi region of Hokkaido, Japan, in 2018, triggering massive landslides. Most of these landslides were shallow and occurred mostly in the Atsuma and Abira towns. Ta-c and Ta-d tephra layers have been found in the Towa landslide at Atsuma from the Tarumai volcano, while Ta-d, En-a, and Spfa-1 tephra layers have been found in the Mizuho landslide at Abira from the Tarumai and Eniwa volcanos, as well as the Shikotsu caldera. Field observations from previous studies revealed that the sliding layers were located in the Ta-d and En-a layers at the Towa and Mizuho landslides, respectively. Unlike previous research on earthquake-induced landslides, which were investigated using mechanical properties, this study investigates the characteristics of physical properties, saturated permeability properties, and content of clay minerals on sliding and surrounding tephra layers. Results from this study reveal that the physical properties of sliding layers from two landslides demonstrated the same characteristics: non-plastic soil with a low density of soil particles, void ratio, and dry density; these characteristics could influence earthquake-induced landslides. It also reveals a relationship between the plasticity chart and the age of tephra materials, including the relationship between the weathering process and density of soil particles and the dissimilarity in characteristics of saturated permeability properties in tephra materials.

Keywords: Earthquake, Physical properties, Shallow landslide, Sliding layer, Tephra materials

Introduction

A 6.6-M_w earthquake struck the Iburi region of Hokkaido, Japan, at 03:08 local time (JST), on September 18th, 2018, triggering multiple shallow landslides. The maximum earthquake intensity of seven occurred in Atsuma Town, triggering landslides across an area of approximately 20 km^2 behind Atsuma (Yamagishi and Yamazaki 2018). According to an inventory of landslides induced by major earthquakes, the number and total area of landslides triggered by this earthquake were the highest in Japan since the Meiji Era (1868–1912) (Osanai et al. 2019). Most landslides were shallow and were mostly classified as planar and spoon types, both of which are similar to rainfall-induced landslides. Several deep-seated dip-slipping type landslides were also exposed in the south-eastern part of the mountains (Osanai et al. 2019; Yamagishi and Yamazaki 2018). The occurrence of landslides in Hokkaido is not frequent; similar seismic events occurred between 4600 and 2500 years ago (Kasai and Yamada 2019; Tajika et al. 2016). Furthermore, undisturbed soil stratigraphy exposed in several landslide scars indicates that these slopes have been stable for more than 9000 years (Kasai and Yamada 2019). Kasai and Yamada (2019) also suggested that the combination of low-elevation relief and tephra layers, which could move very

*Correspondence: goto@yamanashi.ac.jp; goto.satoshi.jp@gmail.com
[2] Faculty of Engineering, Graduate Faculty of Interdisciplinary Research, University of Yamanashi, Kofu, Japan
Full list of author information is available at the end of the article

easily in response to ground shaking, might have caused unexpectedly large numbers and sizes of landslides when an intense earthquake struck this area.

A hypothesis has been presented to explain the numerous landslides in the Hokkaido Eastern Iburi Earthquake. The hypothesis suggested that the typhoon on the previous day could have led to the saturation of pumice strata, which absorb large quantities of water. Hence, this might have triggered a rapid increase in pore pressure in the surficial soils during ground shaking, leading to liquefaction and slope failure (Wang et al. 2019). However, the hourly intensity of the rainfall brought by the typhoon before the earthquake was lower and not enough to trigger a landslide. Zhang et al. (2019) reported persistent rainfall in August, with cumulative rainfall ranging between 101 and 120 mm, which contributed significantly to the occurrence of landslides during the intense ground shaking of the Iburi earthquake. They also observed crushed and liquefied pumice layers spread in the deposition area, resulting in the extension of the upper sliding layer in the horizontal direction. The coseismic landslides were highly mobile and had a long-runout distance because they were crushed and liquefied on the Ta-d layer (Li et al. 2020; Zhang et al. 2019).

The Iburi region has thick tephra deposits from the eruptions of Mounts Tarumai (approximately 9 ka), Eniwa (approximately 20 ka), and the Shikotsu caldera (40 ka) (Minato et al. 1972; Nakagawa et al. 2018; Yamagishi and Yamazaki 2018). Wang et al. (2019) presents an inventory of 7837 coseismic landslides based on the interpretation of the images, covering about 24 km^2 of the disrupted area. Yamagishi and Yamazaki (2018) discovered that tephra layers blanket the region with a depth of 4–12 m and standard penetration test values were less than 10 N, thus indicating that they are unconsolidated, highly compressible, and crushable (Miura 2012).

Early observations (Yamagishi and Yamazaki 2018), distribution of landslides (Kasai and Yamada 2019; Wang et al. 2019), characteristics of landslides (Osanai et al. 2019), and clay mineral content (Chigira et al. 2018; Koyasu et al. 2020) have all been studied in this study region (Chigira et al. 2018; Koyasu et al. 2020). The sliding layer of landslides triggered by the Hokkaido Eastern Iburi Earthquake was predominantly formed near the bottoms of layers consisting of volcanic ash and pumice from the Tarumai volcano (Ta-d); it was also formed in other tephra layers, such as the En-a layer (Kasai and Yamada 2019; Nakagawa et al. 2018; Osanai et al. 2019). Ta-d layers were presumed vulnerable to ground shaking, which reduces cohesion (Kasai and Yamada 2019). Studies on heavy rainfall-induced landslides in tephra have also been observed in the prediction of shallow landslides (Goto and Kimura 2019; Wakai et al. 2019), the distribution of tephra layers (Kimura et al. 2016, 2019), geomorphological setting (Higaki et al. 2019), and strength characteristics of gravitational deformation (Sato et al. 2017, 2019). Generally, observation of the sliding layer on earthquake-induced landslides has been conducted on mechanical properties, such as observation of monotonic and cyclic behavior in the sliding layer (Goto and Okada 2021). Unlike previous research on earthquake-induced landslides, which were investigated using mechanical properties, this study analyzes the physical properties, saturated permeability properties, and content of clay minerals on sliding and surrounding tephra layers of landslides caused by the 2018 Hokkaido Eastern Iburi Earthquake. The physical properties of soil are also observed in the sliding layer in tephra materials on heavy rainfall-induced landslides (Istiyanti et al. 2020), and characteristics of tuff breccia-andesite in diverse mechanisms of landslides (Istiyanti et al. 2021).

Research area

Figure 1 shows the two landslides selected as the research area: one in Atsuma, called the Towa landslide, and another in Abira, called the Mizuho landslide. The distance between the landslides was approximately 12.5 km. The basement rocks for these landslides are marine conglomerates from the Cenozoic, Neogene, Miocene, and late Langhian–Tortonian epochs (GSJ 2020); however, tephra soils are covered in this area. Osanai et al. (2019) reported that during the Hokkaido Eastern Iburi Earthquake, several landslides occurred in the middle reaches of the Atsuma River in Atsuma and the upper reaches of the Shiabira River in Abira (Fig. 2).

In Atsuma, the complete tephra layers from Ta-a to Spfa-1 were observed (Fig. 3). This observation indicated that some tephra layers were derived from the Tarumai volcano, including Ta-a, b (0.3 ka), Ta-c (2.5 ka), and Ta-d (8.7–9.2 ka). Other tephra layers erupted from the Eniwa volcano and the Shikotsu caldera. The En-a and Spfa-1 layers are tephra layers that erupted from the Eniwa volcano (19–21 ka) and Shikotsu caldera (approximately 40 ka), respectively. Tephra deposits in the Towa landslide were derived from the Tarumai volcano, including Ta-c and Ta-d tephra layers. Generally, Ta-d directly overlies the basement complex on slopes along the main channel of the Atsuma River (Osanai et al. 2019). Furthermore, tephra deposits in the Mizuho landslide were derived from the Tarumai volcano (Ta-d), Eniwa volcano (En-a), and Shikotsu caldera (Spfa-1) tephra layers. Furukawa and Nakagawa (2010) and Soya and Sato (1980) reported that buried humus (kuroboku soil) layers are sandwiched between Ta-b and Ta-c and Ta-c and Ta-d. The topsoil layer is generally composed of alternate layers of pyroclastic fall deposits and buried humus, with a

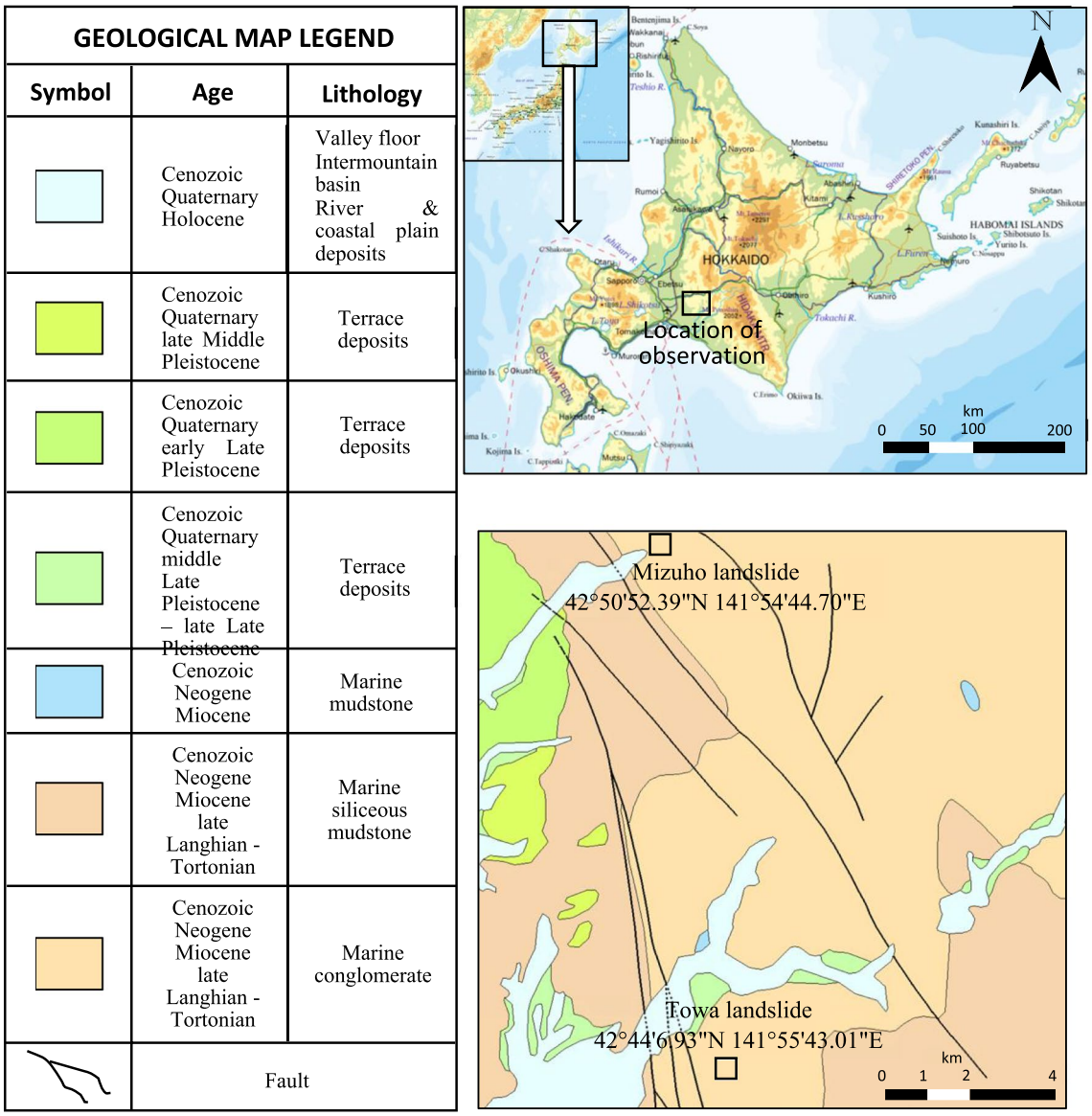

Fig. 1 Location and geological map of research areas (Geology Survey of Japan 2020)

thickness of approximately 2.5–3.5 m in the middle of the slope. This study shows a thin kuroboku layer (0.06 m) as the topsoil in the Towa landslide.

Figure 4 shows the layering of the Towa and Mizuho landslides. The tephra layers from the Tarumai and Eniwa volcanos were divided into two sub-layers: upper (U) and lower (L). In the Towa landslide, the Ta-c layer was divided into Ta-c U and Ta-c L layers because the Ta-c L layer was located near the weathered Ta-d layer and could obtain different characteristics from the Ta-c U layer. Different particles size was observed in the Ta-d layer at the Towa landslide. The Ta-d U layer had a larger particle size than the Ta-d L layer; Li et al. (2020) observed that the Ta-d layer decreases top-down. However, Tajika et al. (2016) reported different events in the Ta-d layer, when the Ta-d U and Ta-d L layers were lithic fragments and pumice fall deposits, respectively. Similar to the tephra layers from the Towa landslide, the Loam (En-a) and En-a layers in the Mizuho landslide were divided into two parts. Furthermore, different particles size was observed in the En-a layer at the Mizuho landslide. The En-a U layer had a finer particle size than the En-a L layer.

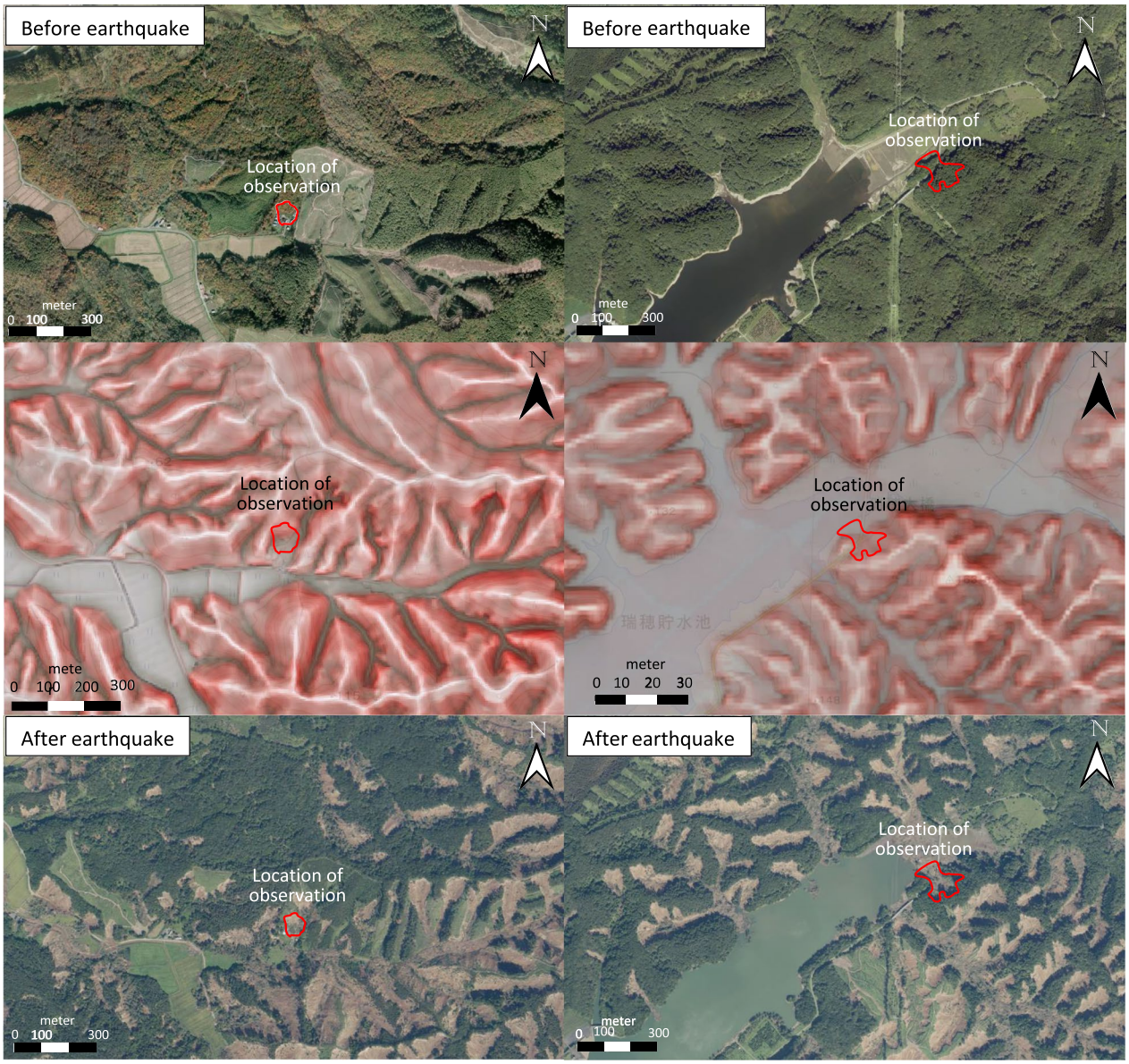

Fig. 2 Photo satellite of Atsuma Town (**a**), Abira Town (**b**) before and after earthquake, and topographic map on research areas before an earthquake (Geospatial Information Authority of Japan 2020)

Research methods

This study includes field measurements and laboratory tests. For the field measurement, soil stratigraphic was observed, and soil hardness was measured. Soil layers were exposed by scraping the surface to observe soil stratigraphic, as shown in Fig. 4. The tephra layers in the Towa landslide were scraped in the stage pattern because of the condition of the field. Soil hardness was measured by inserting a Yamanaka-type soil hardness meter in the exposed soil layer. Furthermore, previous research observed a discontinuity between the strength and soil hardness (Tokunaga and Goto 2017). Disturbed and undisturbed samples were collected from the field; moreover, the undisturbed samples were collected from the center of each soil layer to observe their saturated permeability properties in this study.

Laboratory tests were conducted to observe the physical properties, saturated permeability properties, and content of clay minerals on tephra materials. The tests for

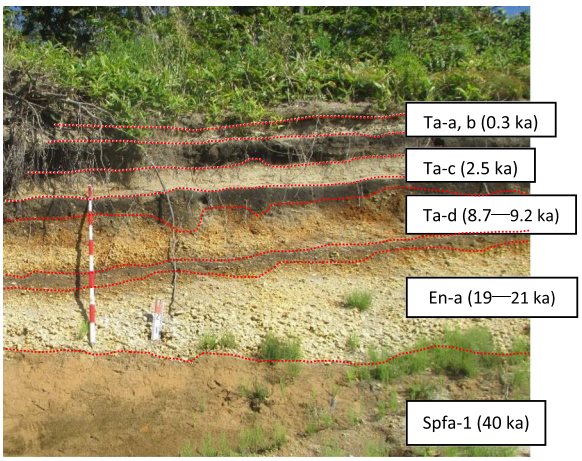

Fig. 3 The tephra layers from Ta-a until Spfa-1 which located nearby the research area (Minato et al. 1972; Nakagawa et al. 2018; Yamagishi and Yamazaki 2018) (Photos taken on September 2019)

the physical properties were conducted according to the laboratory testing standards of Geomaterials Vol. 1 (JGS 2015). Additionally, a particle size distribution test on the tephra layer was performed by sieve and sedimentation analyses on all tephra layers, except the weathered Ta-d and En-a L layers from the Mizuho landslide. Sieve analysis in this study only observed these layers. The test for the saturated permeability properties was performed according to the methods for obtaining the saturated permeability of soils presented by Daiki (DIK-4012). Clay minerals on tephra layers were also observed using X-ray diffraction (XRD) tests which were performed according to the randomly oriented powder mounts, ethylene glycol treatment, and heat treatment methods from the United States Geological Survey (USGS).

Results and discussion

Field observations

The sliding layers from field observation were located in the Ta-d and En-a layers at the Towa and Mizuho landslides, respectively. Figure 5a, b show the soil hardness measurements during field observations. The soil hardness in the Towa landslide indicates that the Ta-c U layer has the lowest average value of soil hardness, whereas the Ta-d U layer has the highest average value of soil hardness. Additionally, the soil hardness in the Mizuho landslide shows that the Loam (Spfa-1) layer has the lowest average value of soil hardness, whereas the weathered En-a layer has the highest average value of soil hardness. However, there was no significant difference in the soil hardness of the sliding layer of both landslides.

Physical properties of tephra layers

The particle size distribution curve (Fig. 6) shows two types of tephra materials: well-graded and poor-graded soil material. Kuroboku, Ta-c L, and Loam (En-a) layers from the Towa landslide, as well as Loam (En-a) U, Loam (En-a) L, and Loam (Spfa-1) layers from the Mizuho landslide contain well-graded soil material. Furthermore, Ta-c U, weathered Ta-d, Ta-d U, and Ta-d L layers from the Towa landslide and weathered Ta-d, En-a U, and En-a L layers from the Mizuho landslide are tephra materials with poor-graded soil material.

Tephra layers trigger complex and peculiar geotechnical engineering challenges in all regions (Miura 2012), and poor-graded soils are more susceptible to soil liquefaction than well-graded soils (Holtz and Kovacs 1981). Moreover, pumice grains in tephra have many open voids within a single grain, and when they are sheared, these voids are initially closed with the fracturing of void walls, then grain fragments float in squeezed water (Chigira and Suzuki 2016). Therefore, because the sliding layers (Ta-d L and En-a) with poor-graded soil material have many open voids, these layers easily collapse during the earthquake.

The physical properties of the tephra layers in the Towa and Mizuho landslides (Fig. 5a, b) indicated a dissimilarity between sliding layers. The density of soil particles on tephra layers in the Towa and Mizuho landslides indicated that the sliding layers show a low density of soil particles. Arthurs (2010) reported that the low density of soil particles on tephra layers made it easier for materials to move in landslides, which tended to create longer runout distances than similar landslides in denser soils. This study observed the low density of soil particles on weathered Ta-d in the Towa and Mizuho landslides. The weathering process in the weathered Ta-d layer was rapid, allowing the density of soil particle value to decrease. Therefore, the density of soil particles could be related to the sliding layer and weathering process in tephra materials.

The physical properties of the tephra layers (Fig. 5a, b) indicated that the plasticity index of the sliding layer in the Towa and Mizuho landslides is non-plastic soil. The non-plastic sliding layer showed that the sliding layer is stiff soil, which could influence earthquake-induced landslides. The liquid and plastic limit test results are also used in the plasticity chart, which classifies the soil materials (Fig. 7), denoted by different colors, while sliding layers on each area are denoted by white circles with different colored outlines. The plotted data on the plasticity chart compares the tephra materials from landslides with tephra materials from Aso volcanic mountain (Istiyanti et al. 2020). Istiyanti et al. (2020) revealed that kuroboku and scoria have different characteristics, whereas the

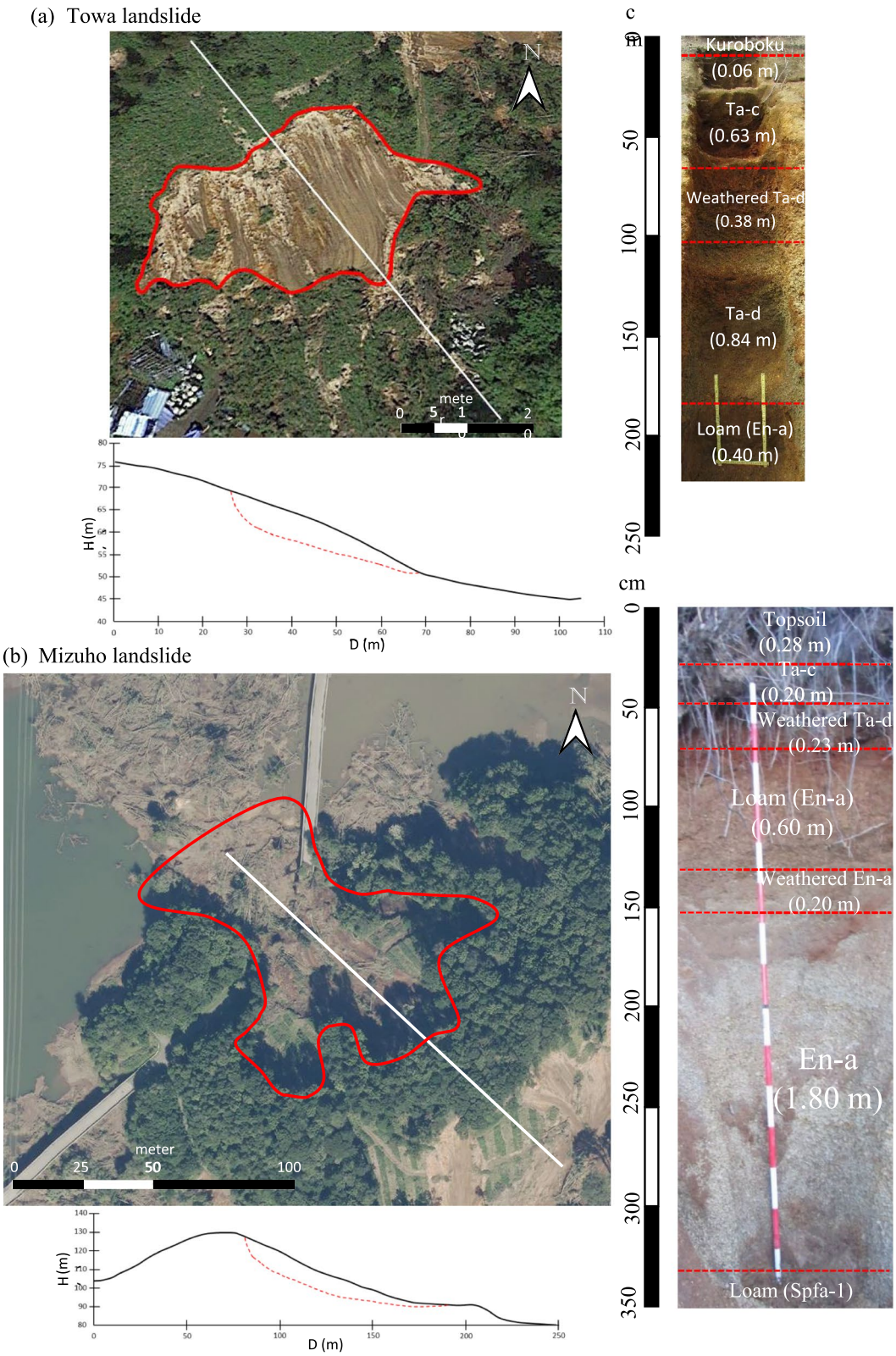

Fig. 4 Plan section and cross section on research areas; **a** Towa landslide, **b** Mizuho landslide (Geospatial Information Authority of Japan 2020)

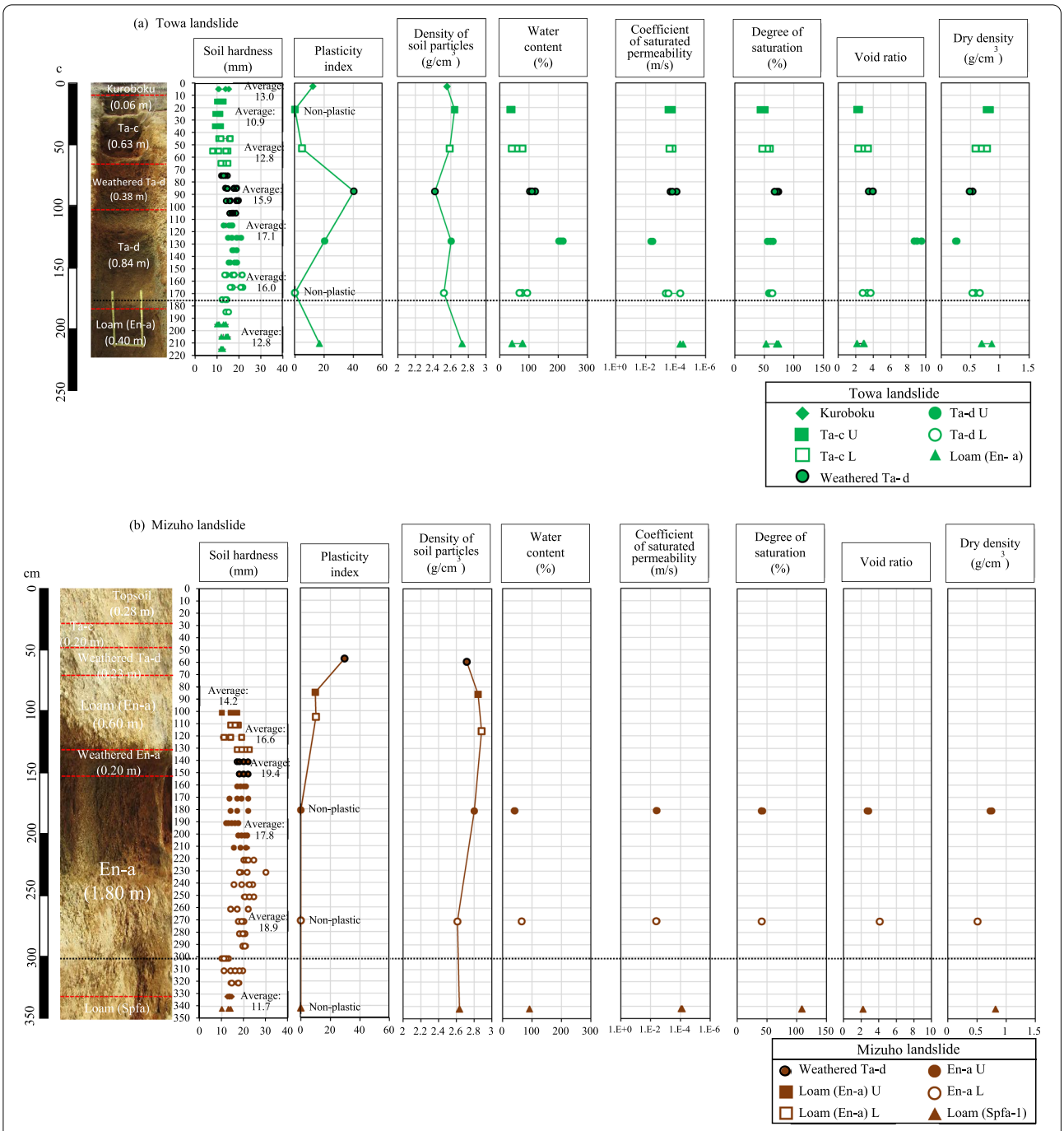

Fig. 5 Soil stratigraphy on the field, soil hardness, physical properties, and saturated permeability properties values in research area with dotted lines indicate sliding layer by field observation; **a** Towa landslide, **b** Mizuho landslide

sliding layers (N3-4 kuroboku (L) layers) have the highest plasticity index and liquid limit values and are plotted in the kuroboku group on the plasticity chart. Therefore, the sliding layers of heavy rainfall-induced landslides on tephra at Aso volcanic mountains have high plasticity, while those of earthquake-induced landslides on tephra at Hokkaido have non-plastic soil.

Furthermore, the plasticity chart divided the tephra materials from the Towa and Mizuho landslides into three types: inorganic silts of medium compressibility and organic silts, inorganic silts of high compressibility

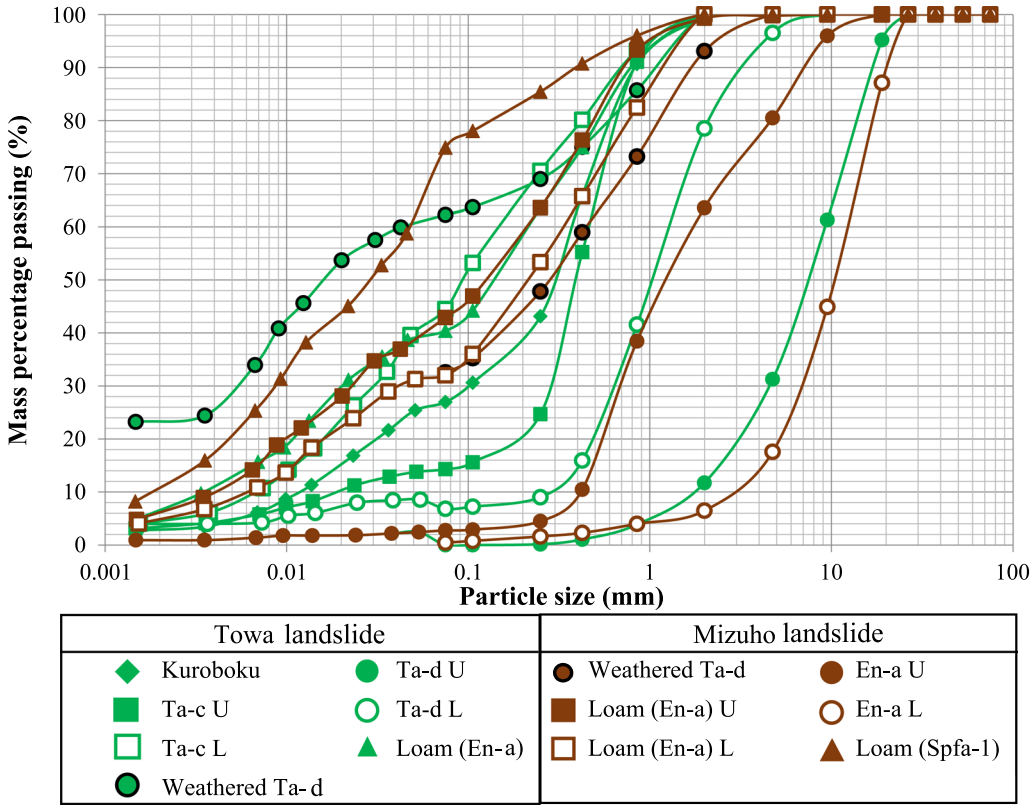

Fig. 6 Particle size distribution curves of tephra materials

organic clays, and non-plastic (NP). The kuroboku and Ta-c L layers from the Towa landslide, including the Loam (En-a) U and Loam (En-a) L layers from the Mizuho landslide, are inorganic silts of medium compressibility and organic silts with lower liquid limit and plasticity index values. Furthermore, weathered Ta-d, Ta-d U, and Loam (En-a) layers from the Towa landslide and weathered Ta-d layer from the Mizuho landslide are inorganic silts of high compressibility and organic clays with higher liquid limit and plasticity index values. The NP group consists of Ta-c U and Ta-d L layers from the Towa landslide and En-a U, En-a L, and Loam (Spfa-1) layers from the Mizuho landslide.

The plotted data on the plasticity chart also shows three groups of tephra materials: scoria (N2 scoria: 1.5 ka and OJS scoria: 3.6 ka), kuroboku, and Ta-d (8.7–9.2 ka); the chart is possibly related to the age of the tephra materials. The scoria group with the youngest age has lower liquid limit and plasticity index values than the Ta-d group. The Ta-c L layer (2.5 ka) was also included in the scoria group because it is almost similar to the scoria. Moreover, the oldest tephra material, the En-a layer, was NP. This study assumed that young tephra materials probably have lower liquid limit and plasticity index values; although the older tephra materials probably have higher liquid limit and plasticity index values, if the tephra materials are very old, they probably do not have plasticity values, i.e., they belong to the NP soil. Unfortunately, a different result was obtained for the Ta-c U layer, which belongs to the NP soil, although the Ta-c U layer was not an old tephra material.

Saturated permeability properties

Figure 5a, b show the saturated permeability properties of the tephra materials. This study measured the saturated permeability properties of each tephra layer from the Towa landslide and on the En-a U, En-a L, and Loam (Spfa-1) layers from the Mizuho landslide. A significant peculiarity was observed in the Ta-d U layer of the Towa landslide. The Ta-d U layer exhibited the highest water content, coefficient of saturated permeability, and void ratio with the lowest dry density value. The different characteristics of saturated permeability in the Ta-d U layer could be related to the different events in the Ta-d layer. Different characteristics of saturated permeability were also observed between the sliding and the under layers. The dissimilarity in the void ratio and dry density indicated that the sliding layers have a loose structure.

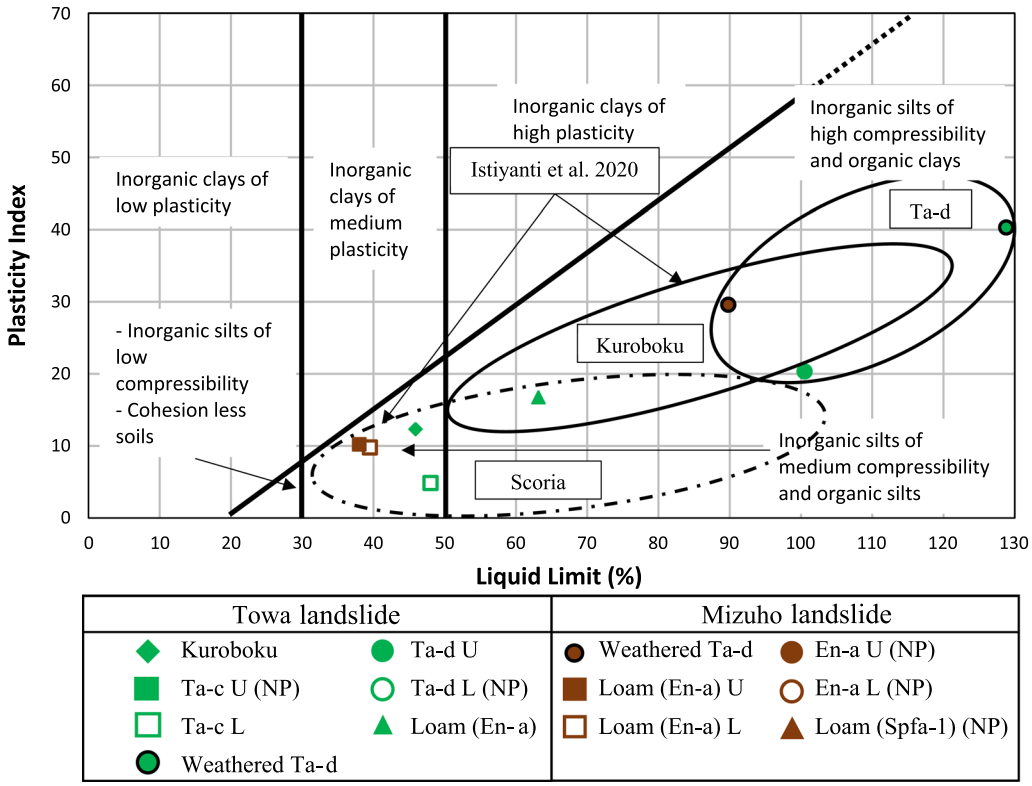

Fig. 7 Ellipse pattern from plotted data of tephra materials in Aso volcanic mountains (Istiyanti et al. 2020) and plotted data of tephra materials from Hokkaido on plasticity chart

Although the pore water pressure did not affect the landslides, the loose structure on the sliding layers could have influenced the landslides. During the earthquake, sliding layers with loose structures easily collapse. Chang et al. (2020) reported that loose materials accumulated on the slopes are more likely to fail during an earthquake.

Furthermore, the relationship between the void ratio and the coefficient of saturated permeability (Fig. 8) indicated the dissimilarity in tephra layers. Although Ta-d layers from the Towa landslide have several void ratios, the Ta-c, En-a, and Loam layers have a narrow range of void ratios. The Ta-d U and En-a layers from the Towa and Mizuho landslides have a considerable coefficient of saturated permeability, respectively. Shimizu and Ono (2016) determined the saturated permeability properties of tephra layers from the Aso volcanic mountain area and reported that the hydraulic conductivity at the layer below the sliding layer in heavy rainfall-induced landslides was decreased, and the difference in hydraulic conductivity affects the tephra layer. Because the landslides in this study were triggered by an earthquake, no differences in hydraulic conductivity were found between the sliding and under layers.

Characteristics of soil physical properties on the sliding layer

The sliding layer on earthquake-induced landslides is a NP soil with a low density of soil particles, void ratio, and dry density. The physical properties of the sliding layer showed that the sliding layer is a stiff soil with a loose structure. Furthermore, the sliding layer on earthquake-induced landslides has a halloysite, which could have affected the layer during the earthquake. This is because the presence of the halloysite indicates that it is potentially weak, which explains the appearance of shrinkage cracks (Moon et al. 2015).

Therefore, the characteristics of the sliding layer on tephra materials in earthquake-induced landslides are stiff soil with a loose structure, and the halloysite content in the sliding layer triggers shrinkage and cracks in the layer. During the earthquake, the loose structure and cracks on the sliding layer could not handle the driving force, i.e., the mass of the upper layers, causing the landslide.

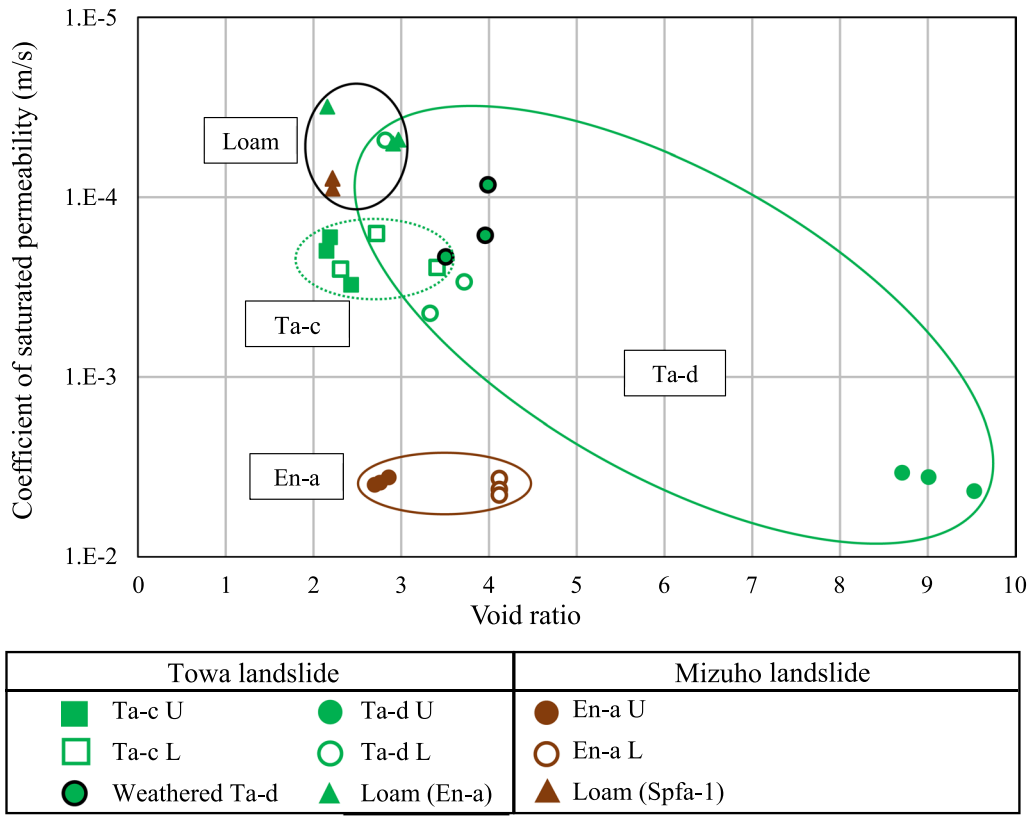

Fig. 8 Correlation between coefficient of permeability (m/s) and void ratio

Content of clay minerals

The USGS (2001) classified clay minerals into seven groups in its laboratory manual for XRD:chlorite, illite, kaolinite, mixed-layer clays, smectite, sepiolite, palygorskite, and vermiculite. The clay minerals in the tephra layers from the Towa landslide generally contained smectite clay minerals (Fig. 9a). Kuroboku layers contain chlorite, illite–smectite, and montmorillonite (smectite group). Furthermore, the Ta-c U, Ta-c L, and Loam (En-a) layers contain montmorillonite (smectite group). The weathered Ta-d layer contains chlorite and montmorillonite (smectite group), and the Ta-d L layer contains halloysite (kaolinite group) and montmorillonite (smectite group). Surprisingly, this peak was not observed in the Ta-d U layer.

The clay minerals in the tephra layers from the Mizuho landslide generally contained smectite and kaolinite clay minerals (Fig. 9b). The weathered Ta-d layer contains illite, chlorite, smectite group (montmorillonite and smectite), and kaolinite group (dickite and halloysite). The Loam (En-a) U layer contains illite, chlorite, montmorillonite (smectite group), and halloysite (kaolinite group). The Loam (En-a) L layer contains illite, chlorite, illite-montmorillonite, montmorillonite (smectite group), and halloysite (kaolinite group). Furthermore, the En-a layer contains illite, chlorite, montmorillonite (smectite group), and kaolinite group (dickite and halloysite).

There was no significant difference in the content of clay minerals in the tephra layers of the Mizuho landslide. Additionally, the Ta-d L layer from the Towa landslide contained a halloysite, whereas other tephra layers in the Towa landslide did not. Chigira et al. (2018) and Koyasu et al. (2020) confirmed the presence of halloysite in tephra layers. Chigira et al. (2018) confirmed that the sliding layer is at the Ta-d layer, which has a halloysite, and that a large amount of water is contained within the halloysite formation.

Conclusion

According to previous studies, the physical properties of sliding layers from two landslides revealed the same characteristics, NP soil with low density of soil particles, void ratio, and dry density, and these characteristics could influence earthquake-induced landslides. Furthermore, the sliding layer contains halloysite, which could have caused cracks. This study revealed that the characteristics of physical properties influence the sliding layer. During the earthquake, the loose structure and cracks in

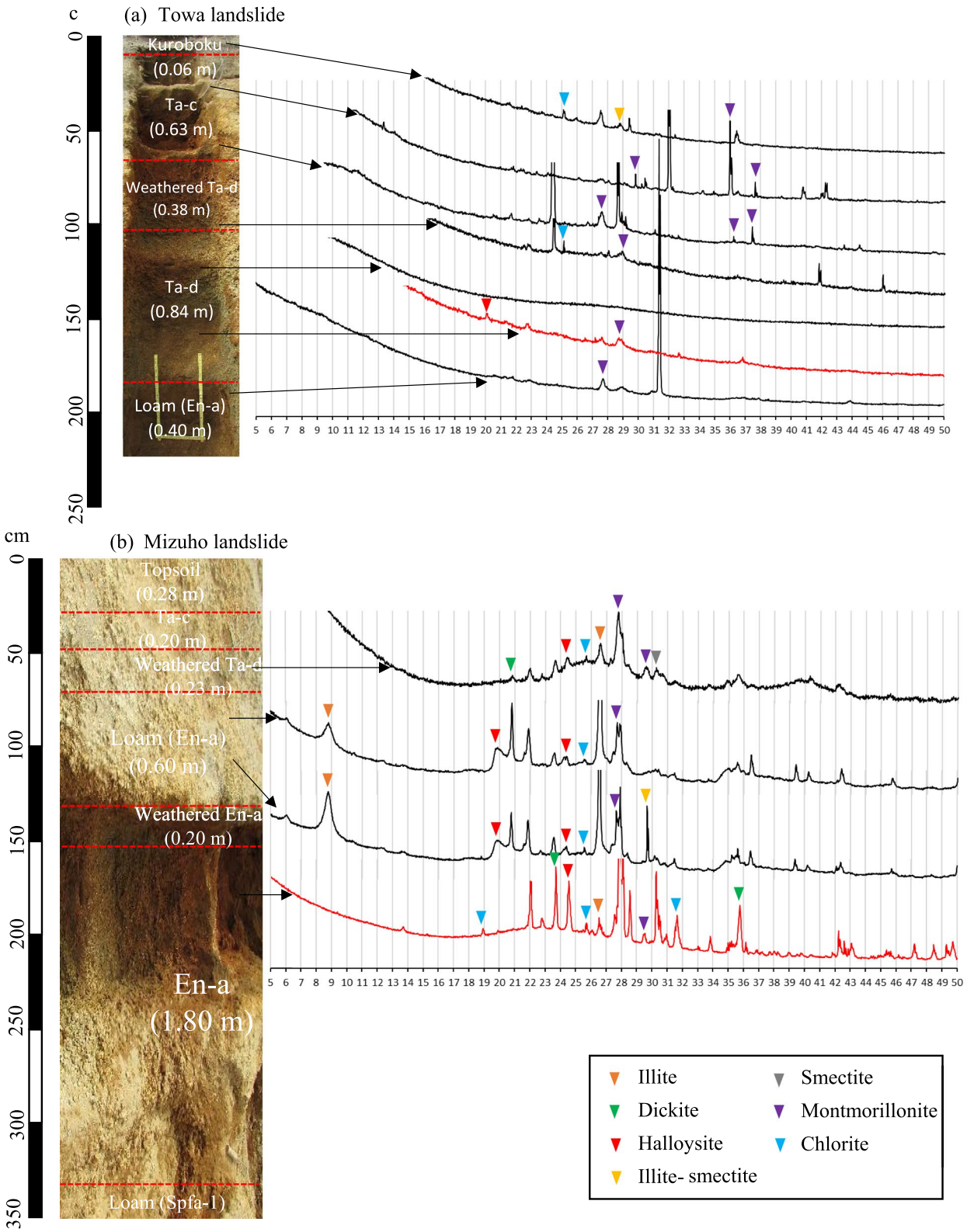

Fig. 9 Clay minerals on tephra materials from Towa and Mizuho landslides

the sliding layer could not handle the driving force, which is the mass of the upper layers, thereby triggering the landslide.

The physical and saturated permeability properties of the Towa landslide also indicated different characteristics of the Ta-d U layer. This phenomenon could be because the different events that formed the particle size on the Ta-d U layer were more significant than those of the other tephra layers. Additionally, there is a possible relationship between the age of the tephra materials and the plasticity index. Young tephra materials have lower liquid limit and plasticity index values than older tephra materials. Furthermore, if the tephra materials are very old, they are probably included in the NP soil. The dissimilarity between the characteristics of the saturated permeability properties was also observed in the tephra layers. This study also indicates the relationship between the weathering process and the density of soil particles. Unfortunately, there was no significant difference in the sliding layer of tephra materials at earthquake-induced landslides in terms of soil hardness value and clay mineral content.

Acknowledgements
The field observations in this study were made possible with the participation of Geotechnical Laboratory members from the University of Yamanashi.

Author contributions
MLI and SG visited the landslide sites and selected a location to expose the soil materials, collected samples, and conducted a field investigation to measure soil hardness. MLI performed physical properties, saturated permeability, and XRD tests. MLI and SG analyzed and interpreted the soil behavior regarding the materials at the landslide sites. Both authors read and approved the final manuscript.

Funding
Part of this study was carried out with the support of the Japan Society for the Promotion of Science Grants-in-Aid for Scientific Research (B) 17H03303 for 2017-2019.

Availability of data and materials
The datasets used and/or analyzed during the study were obtained from the corresponding author upon request.

Declarations

Ethics approval and consent to participate
Not applicable.

Consent for publication
Submission of an article implies that the work described has not been published previously, that it is not under consideration for publication elsewhere. The publication is approved by all authors and tacitly or explicitly by the responsible authorities where the work was carried out. If accepted, it will not be published elsewhere in the same form, in English, or any other language, including electronically without the written consent of the copyright holder.

Competing interests
The authors declare that they have no competing interests.

Author details
[1]Bandung, West Java, Indonesia. [2]Faculty of Engineering, Graduate Faculty of Interdisciplinary Research, University of Yamanashi, Kofu, Japan.

Received: 31 January 2022 Accepted: 30 September 2022
Published online: 14 October 2022

References

Arthurs JM (2010) The nature of sensitivity in rhyolitic pyroclastic soils from New Zealand. Dissertation, University of Auckland

Chang M, Zhou Y, Zhou C, Hales TC (2020) Coseismic landslide induced by the 2018 M_w 6.6 Iburi, Japan, Earthquake: spatial distribution, key factors weight, and susceptibility regionalization. Landslides. https://doi.org/10.1007/s10346-020-01522-3

Chigira M, Suzuki T (2016) Prediction of earthquake-induced landslides of pyroclastic fall deposits. In: Aversa S et al (eds) Landslides and engineered slopes. Experience, theory, and practice. Associazione Geotecnica Italiana, Rome, pp 93–100

Chigira M, Tajika J, Ishimaru S (2018) Formation beds of sliding surface-weathering and clay minerals. Hokkaido University Press, Sapporo **(in Japanese with English abstract)**

Daiki (DIK-4012) (n.d) Manual for soil permeability analysis using an instrument with four points (**in Japanese**)

Furukawa R, Nakagawa M (2010) Geological map of Tarumae volcano. https://gbank.gsj.jp/volcano/Act_Vol/tarumae/index-e.html. Accessed Oct 2020

Geology Survey of Japan. https://gbank.gsj.jp/geonavi/geonavi.php. Accessed Oct 2020

Geospatial Information Authority of Japan. https://maps.gsi.go.jp/. Accessed Oct 2020

Goto S, Kimura T (2019) Introduction of the special issue on "Toward the prediction of shallow landslides induced by heavy rainfalls on tephra-covered slopes." J Jpn Landslide Soc 56:211–217. https://doi.org/10.3313/jls.56.211 **(in Japanese)**

Goto S, Okada K (2021) Monotonic and cyclic behaviour of tephra layer landslide at Takanodai from the 2016 Kumamoto earthquake. In: Tiwari B, Sassa K, Bobrowsky PT, Takara K (eds) Understanding and reducing landslide disaster risk. WLF 2020. ICL contribution to landslide disaster risk reduction. Springer, Cham. https://doi.org/10.1007/978-3-030-60706-7_36

Higaki D, Li X, Hayashi I, Tsou C, Kimura T, Hayashi S, Sato G, Goto S (2019) Geomorphological setting of shallow landslides by heavy rainfall on tephra-covered slopes of Aso volcano, southwest Japan. J Jpn Landslide Soc 56:218–226. https://doi.org/10.3313/jls.56.218 **(in Japanese with English abstract)**

Holtz RD, Kovacs WD (1981) An introduction to geotechnical engineering. Prentice Hall, Englewood Cliffs

Istiyanti ML, Goto S, Kimura T, Sato G, Hayashi S, Wakai A, Higaki D (2020) Sliding layer estimation of shallow landslides on Aso volcanic mountains in Japan based on tephra layer-physical properties of soil. Geoenviron Disasters 7:28. https://doi.org/10.1186/s40677-020-00163-x

Istiyanti ML, Goto S, Ochiai H (2021) Characteristics of tuff breccia-andesite in diverse mechanisms of landslides in Oita Prefecture, Kyushu, Japan. Geoenviron Disasters. https://doi.org/10.1186/s40677-021-00176-0

Kasai M, Yamada T (2019) Topographic effects on the frequency-size distribution of landslides triggered by the Hokkaido Eastern Iburi Earthquake in 2018. Earth Planets Space 71:89. https://doi.org/10.1186/s40623-019-1069-8

Kimura T, Goto S, Sato G, Wakai A, Doshida S (2016) Thickness distribution of pyroclastic fall layers on outer slopes of the caldera rim, Izu Oshima Volcano. J Jpn Landslide Soc 53(2):43–49. https://doi.org/10.3313/jls.53.43 **(in Japanese with English abstract)**

Kimura T, Goto S, Sato G, Wakai A, Hayashi S, Higaki D (2019) Evaluation of landslide susceptibility by slope stability analysis using an estimated distribution of tephra deposits—a case study in the northeastern part of Aso caldera. J Jpn Landslide Soc 56:240–249. https://doi.org/10.3313/jls.56.240 **(in Japanese with English abstract)**

Koyasu H, Ishimaru S, Wang G, Furuya G, Watanabe N, Cai F, Uchimura T, Kimura T (2020) Geological and geotechnical characteristics of sliding layers of landslides introduced by the 2018 Hokkaido Eastern Iburi earthquake. http://www.dpri.kyoto-u.ac.jp/hapyo/20/pdf/D32.pdf. Accessed Nov 2020

Li R, Wang F, Zhang S (2020) Controlling role of Ta-d pumice on the coseismic landslides triggered by 2018 Hokkaido Eastern Iburi Earthquake. Landslides 17:1233–1250. https://doi.org/10.1007/s10346-020-01349-y
Minato M, Hashimoto S, Fujiwara Y, Kumano S, Okada S (1972) Stratigraphy of the Quaternary ash and pumiceous products in Southwestern Hokkaido, N. Japan (The Pliocene and Quaternary Geology of Hokkaido, 1st Report). J Fac Sci Hokkaido Univ Ser 4 Geol Mineral 15(3–4):679–736
Miura S (2012) Mechanical behavior and earthquake-induced failures of volcanic soils in Japan. 2nd ICTG September 10–12, Sapporo, Japan. https://www.eng.hokudai.ac.jp/labo/geomech/tc202conference/paper/Prof.%20Miura.pdf. Accessed Oct 2020
Moon VG, Lowe DJ, Cunningham MJ, Wyatt JB, de Lange WP (2015) Sensitive pyroclastic-derived halloysitic soils in northern New Zealand: interplay of microstructure, minerals, and geomechanics. In: Volcanic rocks and soils—proceedings of the international workshop on volcanic rocks and soils, pp 3–21. https://doi.org/10.1201/b18897-1
Nakagawa M, Amma-Miyasaka M, Tomijima C, Matsumoto A, Hase R (2018) Eruption sequence of the 46 ka caldera-forming eruption of Shikotsu Volcano, inferred from stratigraphy of proximal deposits at South of Lake Shikotsu, Japan. J Geogr 127(2):247–271. https://doi.org/10.5026/jgeography.127.247 **(in Japanese with English abstract)**
Osanai N, Yamada T, Hayashi S, Kastura S, Furuichi T, Yanai S, Murakami Y, Miyazaki T, Tanioka Y, Takiguchi S, Miyazaki M (2019) Characteristics of landslides caused by the 2018 Hokkaido Eastern Iburi Earthquake. Landslides 16:1517–1528. https://doi.org/10.1007/s10346-019-01206-7
Sato G, Goto S, Kimura T, Hayashi S, Istiyanti ML, Komori J (2017) Gravitational deformation as a precursor of the shallow landslide within tephra-covered slope deposits in the Aso caldera, Japan. J Jpn Landslide Soc 54(5):199–204. https://doi.org/10.3313/jls.54.199 **(in Japanese with English abstract)**
Sato G, Wakai A, Goto S, Kimura T (2019) Strength characteristics of gravitationally deformed slope deposits of tephra and kuroboku soils in the Aso caldera, Japan—application of revised vane-shear-cone test for estimating shear strength. J Jpn Landslide Soc 56:250–253. https://doi.org/10.3313/jls.56.250 **(in Japanese with English abstract)**
Shimizu O, Ono M (2016) Relationship of tephra stratigraphy and hydraulic conductivity with slide depth in rainfall-induced shallow landslides in Aso Volcano. Jpn Landslides 13(3):577–582. https://doi.org/10.1007/s10346-015-0666-2
Soya T, Sato H (1980) Geology of the Chitose District Quadrangle Series 1: 50,000. Geol. Surv. Japan, pp 92
Tajika J, Ohtsu S, Inui T (2016) Interior structure and sliding process of landslide body composed of stratified pyroclastic fall deposits at the Apporo 1 archaeological site, southeastern margin of the Ishikari Lowland, Hokkaido, North Japan. J Geol Soc Jpn 122(1):23–35 **(in Japanese with English abstract)**
The Japanese Geotechnical Society (2015) Japanese Geotechnical Society Standards-Laboratory testing standards of geomaterials, vol 1
Tokunaga S, Goto S (2017) Study on measurement of strength discontinuity by digitized Yamanaka soil hardness tester for shallow landslide site at Aso volcano. 52nd Japan Society for Geotechnical Nagoya, July 2017, pp 1935–1936 **(in Japanese)**
US Geological Survey (2001) A laboratory manual for X-ray powder diffraction. https://pubs.usgs.gov/of/2001/of01-041/index.htm. Accessed July 2020
Wakai A, Hori K, Watanabe A, Cai F, Fukazu H, Goto S, Kimura T (2019) A simple prediction model for shallow groundwater level rise in natural slopes based on finite element solutions. J Jpn Landslide Soc 56:227–239. https://doi.org/10.3313/jls.56.227 **(in Japanese with English abstract)**
Wang F, Fan X, Yunus AP, Subramanian SS, Alonso-Rodriguez A, Dai L, Xu Q, Huang R (2019) Coseismic landslides triggered by the 2018 Hokkaido, Japan (M_w 6.6), earthquake: spatial distribution, controlling factors, and possible failure mechanism. Landslides 16:1551–1566. https://doi.org/10.1007/s10346-019-01187-7
Yamagishi H, Yamazaki F (2018) Landslides by the 2018 Hokkaido Iburi-Tobu Earthquake on September 6. Landslides 15:2521–2524. https://doi.org/10.1007/s10346-018-1092-z
Zhang S, Li R, Wang F, Iio A (2019) Characteristics of landslides triggered by the 2018 Hokkaido Eastern Iburi earthquake, Northern Japan. Landslides 16:1691–1708. https://doi.org/10.1007/s10346-019-01207-6

Publisher's Note